nature geoscience

LETTERS

PUBLISHED ONLINE: 14 DECEMBER 2015 | DOI: 10.1038/NGEO2611

Nitrous oxide sinks and emissions in boreal aquatic networks in Québec

C. Soued[1], P. A. del Giorgio[2] and R. Maranger[1]*

Inland waters are important sites of nitrogen processing[1,2], and represent a significant component of the global budget of nitrous oxide[3], a powerful greenhouse gas[4]. Measurements have focused on nitrogen-rich temperate rivers, with low-nitrogen freshwater systems at high latitudes receiving less attention. Here we measured surface water nitrous oxide partial pressures and calculated fluxes across 321 rivers, lakes and ponds in three boreal regions of Québec, Canada. Fluxes to the atmosphere ranged from −23.1 to 115.7 μmol m^{-2} d^{-1}, with high variability among ecosystem types, regions and seasons. Surprisingly, over 40% of the systems sampled were under-saturated in nitrous oxide during the summer, and one region's aquatic network was a net atmospheric sink. Fluxes could not be predicted from the relatively narrow range in nitrogen concentrations, but the aquatic systems acting as sinks tended to have lower pH, higher dissolved organic carbon and lower oxygen concentrations. Given the large variability in observed fluxes, we estimate that high-latitude aquatic networks may emit from −0.07 to 0.20 Tg N_2O-N yr^{-1}. The potential of boreal aquatic networks to act as net atmospheric nitrous oxide sinks highlights the extensive uncertainty in our understanding of global freshwater nitrous oxide budgets.

Inland waters receive and retain disproportionately large amounts of nitrogen (N) relative to their global surface area[1,5], and are therefore considered significant components of the global nitrous oxide (N_2O) budget[4,6]. However, our understanding of freshwater N_2O fluxes remains fragmented, with limited knowledge of the relative contribution of lentic and lotic systems, and with a bias towards N-rich rivers and streams located in temperate regions. A wide range in N_2O fluxes has been reported for streams, rivers and lakes (Supplementary Tables 5 and 6), yet no clear large-scale pattern has been identified. Although N_2O efflux tends to increase with N inputs[7–11], this trend is often weak or non-existent, particularly across systems and at narrow N gradients[12,13]. However, current regional and global estimates of freshwater N_2O fluxes assume a linear increase of N_2O emissions with dissolved inorganic nitrogen (DIN) loading to rivers[4,6,14]. Model uncertainty arises, among other factors, from the application of a fixed N_2O yield (unit of N_2O produced per N processed), whereas measured yields span two orders of magnitude (0.0002 to 0.07; refs 12,15). This range in yield highlights the complexity of the microbial processes regulating aquatic N_2O production and consumption. Thus, to improve our global estimates of aquatic N_2O emissions, it is necessary to understand how N_2O dynamics vary among aquatic ecosystems and landscape types, especially in water-rich areas such as the boreal biome.

In this study we present the first cross-ecosystem, cross-regional and seasonal patterns of boreal aquatic N_2O emissions. We report N_2O concentrations and fluxes for 321 lakes, ponds and rivers in three distinct boreal landscapes. These aquatic systems had generally low nutrient concentrations but varied widely in terms of water chemistry and morphometry, covering the range of watershed properties that exist across boreal networks (Supplementary Tables 1–3). Measured surface water ΔN_2O concentrations (deviation from saturation) varied between −5.1 and 18.5 nmol l^{-1}, and the associated fluxes varied between −23.1 and 115.7 μmol m^{-2} d^{-1} (average 3.3 μmol m^{-2} d^{-1}; Supplementary Tables 2 and 3). N_2O fluxes could not be effectively predicted by linear regression with measured environmental variables ($R^2 < 0.13$ in all cases; Supplementary Table 4), including lake size and stream order (Supplementary Fig. 2). Overall, N_2O flux did not co-vary strongly with any of the N forms measured (Supplementary Table 4), as opposed to previous reports[7,8,10,11], and contrary to the assumption underlying modelled N_2O budgets[4,6]. This could be due to the relatively narrow range and typically low N concentrations in these boreal landscapes.

General cross-system and regional patterns, however, could be elucidated. N_2O fluxes were higher and more variable in lakes compared to rivers in two of the three sampled regions (Saguenay and Schefferville), whereas ponds were generally neutral features on the landscape (Fig. 1). When comparing these two regions, the mean summer N_2O flux was significantly lower in all ecosystem types in Schefferville (Fig. 1), the region with lowest average nutrient and dissolved organic carbon (DOC) concentrations (Supplementary Table 2). Interestingly, 40% of the systems sampled in summer were under-saturated in N_2O, with most of these occurring in Côte-Nord (Fig. 1 and Table 1), despite this region having the highest average total nitrogen (TN) and ammonium (NH_4^+) concentrations (Supplementary Table 2). In Côte-Nord, lakes acted primarily as atmospheric sinks (Fig. 1).

ΔN_2O depends on the balance between production and consumption of N_2O by nitrification and denitrification. Nitrification, the oxidation of NH_4^+ to nitrate (NO_3^-), releases N_2O as a by-product, whereas denitrification (NO_3^- reduction) can either produce N_2O or transform it to N_2 in a final reaction favoured under highly reduced anoxic conditions[16]. Côte-Nord lakes that behaved predominantly as N_2O sinks tended to have lower pH and higher DOC concentrations than other regions (Fig. 2a). Indeed, results from a classification tree analysis show that lakes tend to act as sinks when pH is <6.27 and DOC is >7.49 mg l^{-1} (Fig. 2b). Low pH may limit nitrification rates[17], and by extent NO_3^- supply for denitrification, thus reducing N_2O production from both reactions.

[1]Groupe de Recherche Interuniversitaire en Limnologie et en Environnement Aquatique, Département des Sciences Biologiques, Université de Montréal, C.P. 6128 succ. Centre-ville, Montréal, Québec H3C 3J7, Canada. [2]Groupe de Recherche Interuniversitaire en Limnologie et en Environnement Aquatique, Département des Sciences Biologiques, Université du Québec à Montréal, Montréal, Québec H3C 3P8, Canada. *e-mail: r.maranger@umontreal.ca

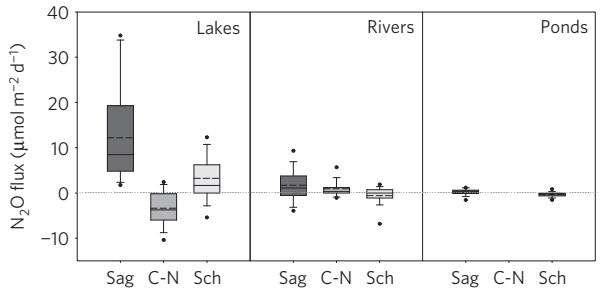

Figure 1 | N_2O flux rates for lakes, rivers and ponds sampled in Saguenay (Sag), Côte-Nord (C-N) and Schefferville (Sch). Boxes are bounded by the 25th and 75th percentiles and show median (solid lines) and mean (dotted lines). Whiskers show 10th and 90th percentiles. Dots are outliers between the 5th and the 95th percentiles.

The negative correlation between pH and NH_4^+ concentration in our lakes (Supplementary Fig. 3) supports this hypothesis. Furthermore, high DOC concentrations stimulate heterotrophic processes such as respiration and denitrification, generating conditions of low O_2 and NO_3^- that favour N_2O consumption[7,11,18].

In the Saguenay and Schefferville regions, N_2O under-saturation was more frequent in rivers and ponds than in lakes, where only 12% acted as N_2O sinks, compared to 45 and 66% for rivers and ponds, respectively (Table 1). Rivers and ponds, owing to their high water–sediment contact, are characterized by lower dissolved oxygen (DO) and higher DOC concentrations (Fig. 2c and Supplementary Table 2), which are conducive to highly reduced conditions, favourable for N_2O consumption, particularly in N-poor systems. Indeed, the classification tree analysis shows that systems with DO $<7.80\,mg\,l^{-1}$ acted predominantly as sinks (Fig. 2d). Lake water is typically more isolated from sediments, the major hotspot for complete denitrification[16]. Thus, the net N_2O balance of lakes could be driven by production via water column nitrification, as observed in oceans[19], or incomplete denitrification. Although still hypothetical, the relative importance of nitrification and denitrification in N_2O production and consumption may explain differences in net flux among freshwater types.

Although net N_2O uptake was observed in all regions, the relative magnitude differed substantially. We calculated that, during the summer, N_2O uptake equalled less than 1% of total aquatic N_2O emissions in Saguenay (Table 1). In contrast, the estimated offset reaches 20% in Schefferville and, in the case of Côte-Nord, the surface water network acted as an overall net sink for atmospheric N_2O (Table 1). Soil surface N_2O uptake has been recently highlighted as significant in regional budgets[20], whereas uptake in aquatic systems has occasionally been reported, often coinciding with low DIN and O_2 concentrations[7,11,18]. However, ours is the first study to show the extent of this phenomenon at a regional scale. Our findings suggest that relatively pristine inland waters may often act as N_2O sinks and that the anthropogenic increase in N loads to aquatic systems[1,2] may have resulted in a broader shift of inland waters towards net sources than previously thought.

ΔN_2O concentrations exhibited a strong seasonal variability in all ecosystem types in the Saguenay region, where samples were collected throughout the year (Supplementary Table 3). Highest ΔN_2O concentrations were measured during winter, suggesting that N_2O is produced and accumulates under the ice. NH_4^+ and NO_3^- were also highest during winter (Supplementary Table 3), most likely owing to ammonification combined with nitrification and negligible phytoplankton uptake owing to low-light conditions[21]. Outgassing of the accumulated N_2O after ice thaw was estimated to average 0.67 (±0.26) and 0.01 (±0.002) mmol m^{-2} for lakes and rivers, respectively. This early spring efflux of winter-derived N_2O fuels up to 15% of annual freshwater emissions in Saguenay. Overall, most of the annual aquatic emissions were observed in the fall (>50%), whereas only 25% of the total was emitted during summer (Supplementary Fig. 3). Thus, boreal inland waters seem to follow a different seasonal cycle compared to temperate fresh waters, where N_2O fluxes are apparently systematically higher in the summer[9,22,23].

We estimate that on an annual basis, lakes were responsible for over 95% of aquatic N_2O emissions in Saguenay (Table 2), whereas rivers contributed less than 5%, and ponds contributed negligibly. For other regions, lakes were also the major drivers of net freshwater N_2O flux, either as sources or sinks during the summer (Table 2). The dominant role of lakes in regional N_2O dynamics is primarily due to the large surface area they occupy in the boreal landscape (Supplementary Table 1). These regional flux budgets differ from the commonly accepted assumption that rivers are the major aquatic N_2O emitters, and also highlight the potential

Table 1 | Mean summer flux rates among ecosystem type (per unit of aquatic area) sorted based on the direction of flux: atmospheric sinks (net uptake) and sources (net emissions).

	Sinks			Sources		
	Mean flux rate (μmol m^{-2} d^{-1})	*n*	Regional flux (mol km^{-2})	Mean flux rate (μmol m^{-2} d^{-1})	*n*	Regional flux (mol km^{-2})
Saguenay						
Lakes	0.0	0	0.0	12.2	39	133.8
Rivers	−3.3	13	−1.0	4.8	26	2.9
Ponds	−0.5	7	0.0	0.6	10	0.0
Sum of fresh waters	-	20	−1.0	-	75	136.7
Schefferville						
Lakes	−3.4	12	−7.2	4.9	47	41.2
Rivers	−2.4	30	−0.7	1.3	27	0.4
Ponds	−0.5	14	−0.4	0.8	1	0.0
Sum of fresh waters	-	56	−8.3	-	75	41.6
Côte-Nord						
Lakes	−5.1	35	−28.7	2.0	11	3.6
Rivers	−0.7	18	−0.2	1.8	31	0.9
Sum of fresh waters	-	53	−28.9	-	42	4.5

Regional summer fluxes (per unit of landscape area) are calculated by scaling the mean flux rates relative to the proportion of sinks versus sources of systems sampled to the surface area of each ecosystem type in the different landscapes.

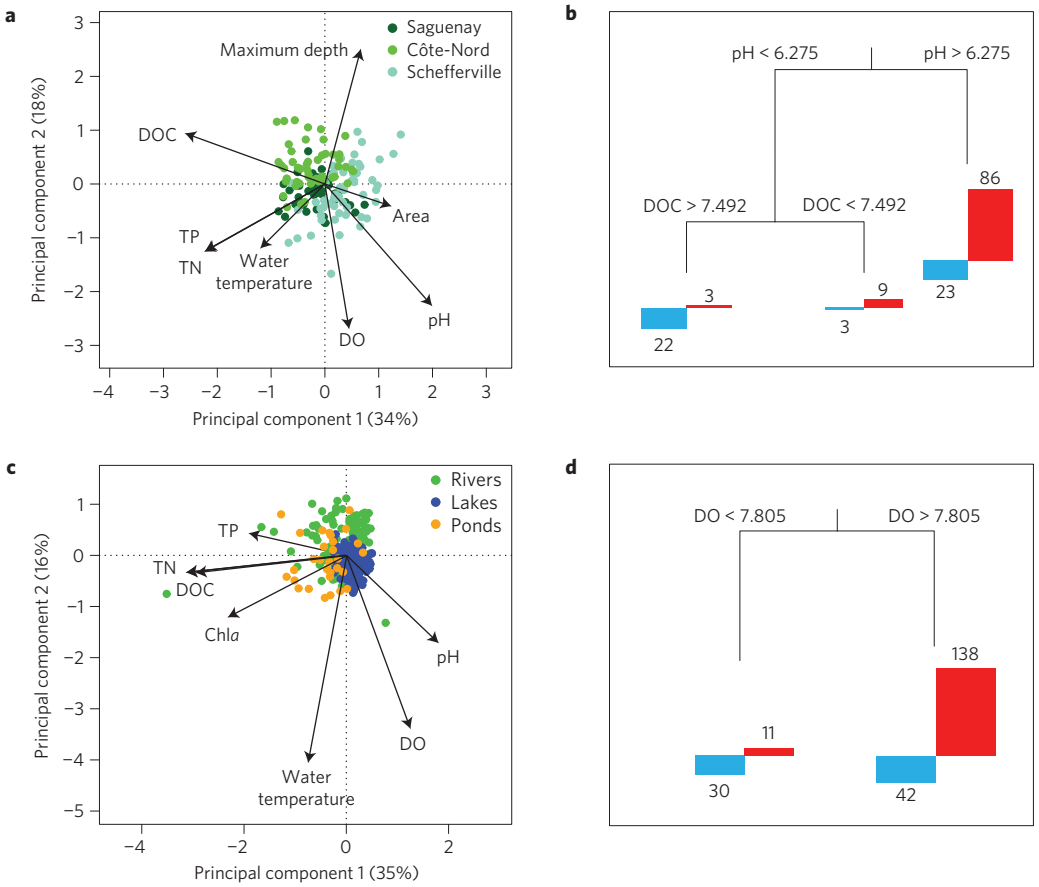

Figure 2 | N_2O flux as a function of environmental variables. a,**c**, Principal component analysis biplots of lakes (**a**) and all systems (**c**), relative to DOC, TN, total phosphorus (TP), DO, chlorophyll *a*, maximum depth, surface area, pH and water temperature for summer sites. Percentage of variance reported on axes. **b**,**d**, Classification trees predicting N_2O flux direction in lakes (**b**) and all systems (**d**), Côte-Nord excluded. Leaves of terminal nodes report the number of N_2O sources (red) and sinks (blue). DOC and DO are in mg l^{-1}. Cross-validated relative error and variability explained are, respectively, 0.74 and 40% in **c**, and 0.77 and 27% in **d**.

Table 2 | Seasonal and annual N_2O flux (±standard error) (all units are in mol N_2O km^{-2} of landscape) by freshwater type and region.

	Saguenay				Schefferville	Côte-Nord
	Spring	Summer	Fall	Annual	Summer	Summer
Lakes	118 (±50)	134 (±19)	262 (±104)	514 (±223)	33 (±7.8)	−25 (±5.6)
Rivers	4.9 (±1.6)	1.5 (±0.6)	12.7 (±3.5)	19.1 (±7.2)	−0.4 (±0.32)	0.9 (±0.37)
Ponds	0.02 (±0.02)	0.01 (±0.02)	0.13 (±0.03)	0.16 (±0.08)	−0.2 (±0.06)	n/a
Sum of fresh waters	123 (±51)	135 (±19)	275 (±108)	533 (±230)	32 (±8.2)	−24 (±6.0)

bias resulting from the exclusion of lakes in regional aquatic N_2O budgets, especially in lake-rich areas. Interestingly, although boreal rivers and ponds are modest contributors to total freshwater N_2O emissions, they emit proportionally large amounts of CO_2 and CH_4 (ref. 24), suggesting that N and C greenhouse gas emissions are decoupled in these systems.

Despite the broad spatial and ecosystem coverage of our study, regional estimates of aquatic N_2O fluxes for boreal and subarctic landscapes will remain uncertain given the wide range in average regional N_2O fluxes observed, and the absence of strong empirical relationships for more effective upscaling. Nevertheless, extrapolating our range in average fluxes to high-latitude aquatic surfaces (>54° N) using mean values from Saguenay and Côte-Nord as upper and lower bounds, respectively, results in a large potential range of −0.07 to 0.20 Tg N (N_2O) yr^{-1} from this region. To put these results into context, we collected all available N_2O measurements from the literature, and calculated mean fluxes per ecosystem type across latitudes (Supplementary Tables 5 and 6). Scaling these averages to the total latitudinal aquatic surface yielded a first-order global estimate of 0.78 Tg N (N_2O) yr^{-1} (Table 3). We acknowledge this literature-based global estimate as highly uncertain, as the extant database is extremely small (<300 systems), has a temperate latitude bias (90% of reports) and numerous other information gaps (Table 3, see Supplementary Information). Nevertheless, it enables us to place our boreal estimates in the broader framework of the existing information on global freshwater N_2O emissions.

In this regard, our study essentially doubles the global freshwater N_2O database and greatly improves the coverage of the vast boreal biome, which is at present under-represented in both the global data set and existing N_2O models. Combining our estimates with published data extends potential global freshwater N_2O emissions

Table 3 | Average freshwater flux rates (flux rate, in μmol m^{-2} d^{-1} (per unit of aquatic area)) and annual flux (Ann. flux (±standard error), in Tg N (N_2O) yr^{-1}) estimated by applying mean rates to open water areas (in 10^3 km^2) in different latitudes.

	Lakes and reservoirs					Rivers and streams					Sum of open water		
	Flux rate	*n*	CV	Ann. flux	Area	Flux rate	*n*	CV	Ann. flux	Area	*n*	Ann. flux	Area
Literature value													
High latitudes (>54°)	1.1	14	149	0.022 (±0.009)	1,983	1.7*	-		0.002* (±0.001)	119	14	0.024 (±0.009)	2,102
Temperate (25°–54°)	3.4	137	1,101	0.050 (±0.047)	1,447	129.0	133	676	0.082 (±0.048)	62	270	0.132 (±0.095)	1,509
Tropical (<24°)	64.7	6	117	0.510 (±0.244)	772	60.8	15	149	0.110 (±0.042)	177	21	0.620 (±0.286)	949
Regional values of this study applied to high latitudes†													
Saguenay	9.4	50	129	0.191 (±0.035)		6.0	41	131	0.007 (±0.001)		91	0.199 (±0.037)	
Schefferville	3.2	59	184	0.065 (±0.002)		−0.6	57	676	−0.001 (±10^{-4})		116	0.065 (±0.002)	
Côte-Nord	−3.4	46	126	−0.069 (±0.002)		0.9	49	292	0.001 (±5 × 10^{-5})		95	−0.067(±0.002)	
Average	3.3	155	292	0.066 (±0.005)		1.7	147	335	0.002 (±0.001)		302	0.068 (±0.007)	
Global estimates based on:													
Literature values		157		0.583 (±0.300)	4,202		148		0.194 (±0.091)	358	305	0.776 (±0.391)	4,560
Regional values of this study applied to high latitudes†													
Upper bound		193		0.752 (±0.326)			189		0.199 (±0.092)		91	0.951 (±0.418)	
Lower bound		189		0.492 (±0.293)			197		0.193 (±0.090)		95	0.684 (±0.383)	
Average		298		0.627 (±0.296)			295		0.194 (±0.292)		302	0.820 (±0.389)	

Literature values represent the average of previously reported flux measurements (Supplementary Tables 5 and 6). *n* and CV (%) represent the number of systems and the variation coefficient, respectively. *To our knowledge no published empirical data of fluxes from high-latitude river or streams exist, thus we applied our measured mean to rivers in these regions for a more complete global estimate. †We applied our regional means to latitudes >54°. However, note that our data are derived from true boreal regions but are located between 47° and 58° N.

to a range of 0.68 to 0.95 Tg N (N_2O) yr^{-1} (Table 3). This range falls between the previously modelled values of 1.1 Tg N (N_2O) yr^{-1} reported in ref. 6 for inland waters and 0.6 Tg N (N_2O) yr^{-1} reported in ref. 4 for global anthropogenic aquatic emissions including estuaries and coasts. Despite the limitations in these current global estimates, our results clearly demonstrate the importance of high-latitude surface waters in shaping the global inland aquatic N_2O budget, both as sources and as sinks of N_2O. Our study further highlights the dynamic nature of N_2O fluxes in low-N environments; however, current models do not effectively capture this variability, nor can they identify sites of N_2O uptake. Indeed the high degree of variability in aquatic N_2O fluxes observed for the boreal biome probably exists in other water-rich regions of the world yet to be so intensively studied. This variability needs to be quantified, and its main drivers identified, if we are to improve our understanding of the contribution of inland water to the global N_2O budget, and how this contribution might be altered under scenarios of future environmental change.

Methods

Methods and any associated references are available in the online version of the paper.

Received 27 May 2015; accepted 30 October 2015; published online 14 December 2015

References

1. Seitzinger, S. *et al.* Denitrification across landscapes and waterscapes: A synthesis. *Ecol. Appl.* **16,** 2064–2090 (2006).
2. Harrison, J. A. *et al.* The regional and global significance of nitrogen removal in lakes and reservoirs. *Biogeochemistry* **93,** 143–157 (2008).
3. Ivens, W., Tysmans, D. J. J., Kroeze, C., Lohr, A. J. & van Wijnen, J. Modeling global N_2O emissions from aquatic systems. *Curr. Opin. Environ. Sustain.* **3,** 350–358 (2011).
4. Ciais, P. *et al.* in *Climate Change 2013: The Physical Science Basis* (eds Stocker, T. F. *et al.*) 465–570 (IPCC, Cambridge Univ. Press, 2013).
5. Boyer, E. W. *et al.* Riverine nitrogen export from the continents to the coasts. *Glob. Biogeochem. Cycles* **20,** GB1S91 (2006).
6. Seitzinger, S. P., Kroeze, C. & Styles, R. V. Global distribution of N_2O emissions from aquatic systems: Natural emissions and anthropogenic effects. *Chemosphere* **2,** 267–279 (2000).
7. Stow, C. A., Walker, J. T., Cardoch, L., Spence, P. & Geron, C. N_2O emissions from streams in the Neuse River watershed, North Carolina. *Environ. Sci. Technol.* **39,** 6999–7004 (2005).
8. Clough, T. J., Buckthought, L. E., Casciotti, K. L., Kelliher, F. M. & Jones, P. K. Nitrous oxide dynamics in a braided river system, New Zealand. *J. Environ. Qual.* **40,** 1532–1541 (2011).
9. Beaulieu, J. J., Shuster, W. D. & Rebholz, J. A. Nitrous oxide emissions from a large, impounded river: The Ohio River. *Environ. Sci. Technol.* **44,** 7527–7533 (2010).
10. Baulch, H. M. *et al.* Night and day: Short-term variation in nitrogen chemistry and nitrous oxide emissions from streams. *Freshwat. Biol.* **57,** 509–525 (2012).
11. Baulch, H. M., Schiff, S. L., Maranger, R. & Dillon, P. J. Nitrogen enrichment and the emission of nitrous oxide from streams. *Glob. Biogeochem. Cycles* **25,** GB4013 (2011).
12. Beaulieu, J. J. *et al.* Nitrous oxide emission from denitrification in stream and river networks. *Proc. Natl Acad. Sci. USA* **108,** 214–219 (2011).
13. Whitfield, C. J., Aherne, J. & Baulch, H. M. Controls on greenhouse gas concentrations in polymictic headwater lakes in Ireland. *Sci. Total Environ.* **410,** 217–225 (2011).
14. Baron, J. S. *et al.* The interactive effects of excess reactive nitrogen and climate change on aquatic ecosystems and water resources of the United States. *Biogeochemistry* **114,** 71–92 (2013).
15. McCrackin, M. L. & Elser, J. J. Greenhouse gas dynamics in lakes receiving atmospheric nitrogen deposition. *Glob. Biogeochem. Cycles* **25,** GB4005 (2011).
16. Seitzinger, S. P. Denitrification in freshwater and coastal Marine ecosystems: Ecological and geochemical significance. *Limnol. Oceanogr.* **33,** 702–724 (1988).
17. Beman, J. M. *et al.* Global declines in oceanic nitrification rates as a consequence of ocean acidification. *Proc. Natl Acad. Sci. USA* **108,** 208–213 (2011).
18. Jacinthe, P. A., Filippelli, G. M., Tedesco, L. P. & Raftis, R. Carbon storage and greenhouse gases emission from a fluvial reservoir in an agricultural landscape. *Catena* **94,** 53–63 (2012).
19. Freing, A., Wallace, D. W. R. & Bange, H. W. Global oceanic production of nitrous oxide. *Phil. Trans. R. Soc. B* **367,** 1245–1255 (2012).
20. Syakila, A., Kroeze, C. & Slomp, C. P. Neglecting sinks for N_2O at the Earth's surface: Does it matter? *J. Integrat. Environ. Sci.* **7,** 79–87 (2010).
21. Knowles, R. & Lean, D. R. S. Nitrification—a significant cause of oxygen depletion under winter ice. *Can. J. Fish. Aquat. Sci.* **44,** 743–749 (1987).
22. Raymond, P. A. & Cole, J. J. Gas exchange in rivers and estuaries: Choosing a gas transfer velocity. *Estuaries* **24,** 312–317 (2001).
23. Rosamond, M. S., Thuss, S. J. & Schiff, S. L. Dependence of riverine nitrous oxide emissions on dissolved oxygen levels. *Nature Geosci.* **5,** 715–718 (2012).
24. Campeau, A. & del Giorgio, P. A. Patterns in CH_4 and CO_2 concentrations across boreal rivers: Major drivers and implications for fluvial greenhouse emissions under climate change scenarios. *Glob. Change Biol.* **20,** 1075–1088 (2013).

Acknowledgements

This study was funded by Natural Sciences and Engineering council of Canada (NSERC) Discovery grants to R.M. and P.A.d.G, and by Hydro-Québec, and is part of the research programme of the NSERC/HQ Industrial Research Chair in Carbon Biogeochemistry in Boreal Aquatic Systems (CarBBAS) associated with P.A.d.G. We wish to thank the many field assistants and students from the CarBBAS chair and R.M. research team for providing generous help and valuable scientific insights on the project. We thank Annick St-Pierre and A. Parkes for coordinating, respectively, field sampling and laboratory analysis. We also thank R. Hutchins and A. Heathcote, who performed part of the spatial analysis. This is a contribution to the Groupe de Recherche Interuniversitaire en Limnologie et en Environnement Aquatique (GRIL). Data will be made available upon request.

Author contributions

R.M. and P.A.d.G. conceptualized the study, C.S. and P.A.d.G. conducted the sampling, C.S. performed the analysis, and all authors contributed to the writing.

Additional information

Supplementary information is available in the online version of the paper. Reprints and permissions information is available online at www.nature.com/reprints. Correspondence and requests for materials should be addressed to R.M.

Competing financial interests

The authors declare no competing financial interests.

Methods

Sampling sites. The three study regions are located between the southern boreal limit (Saguenay, 47° N) and the tundra (Schefferville, 58° N) of Québec (Canada), and represent an area of approximately 700,000 km^2 (Supplementary Fig. 1). The regions are distinct in terms of topography, vegetation cover, climate, and in the configuration of their aquatic network (Supplementary Table 1). We sampled a broad range of systems reflecting the diversity of shape and size observed in the boreal landscape. Lakes ranged from 0.01 to greater than 100 km^2, and were from 0.5 to more than 70 m deep, whereas ponds, primarily resulting from beaver dams, were defined as small and shallow standing waters (generally smaller than 0.01 km^2 and between 1 and 2 m deep). Streams and rivers ranged from Strahler order 1 to 8. Lakes were sampled at their deepest point, and streams and ponds, from the shore. Sampling occurred from 2011 to 2013 (Supplementary Table 1), and all of the systems were sampled at least once during mid-summer (July–August) during the day. A subset of sites was also visited in spring, fall and winter in the Saguenay region (Supplementary Table 3). Water was collected under the ice during winter, but no flux measurements were made.

N_2O concentrations and flux. Surface water partial pressures of N_2O (pN_2O) were measured using the headspace technique. A glass serum bottle of 1.12 l was filled with water collected at wrist depth. A headspace of atmospheric air of 0.12 l was created inside the sealed bottle and gas equilibrium was achieved by vigorously shaking the bottle for two minutes. Air was extracted from the bottle with an airtight syringe and injected in previously evacuated 9 ml glass vial capped with an air-tight butyl seal. Three analytical replicates were taken at each site as well as a local sample of atmospheric air. Collected gas samples were analysed by gas chromatography using a Shimadzu GC-2040, with a Poropaq Q column to separate gases and an electron capture detector. Gas flux (f_{N_2O}) was calculated using the following equation[25]:

$$f_{N_2O} = k_{N_2O}(C_{water} - C_{air}) \quad (1)$$

where k_{N_2O} is the gas exchange coefficient for N_2O (m d^{-1}), C_{water} the water N_2O concentration, and C_{air} is the ambient air concentration. C_{water} and C_{air} are corrected for local temperature and atmospheric pressure. k_{N_2O} was derived from the k_{CO_2}, which was measured at all sites and times of sampling. k_{CO_2} was measured using a round, 16 l floating chamber (0.09 m^2), equipped with an internal thermometer to correct for internal temperature changes during deployment[24]. The ambient p_{CO_2} in the chamber was recorded every minute for 10 min with an Environmental Gas Analyser (EGM-4) connected to the chamber via an enclosed recirculating system. CO_2 fluxes, f_{CO_2}, (mmol m^{-2} d^{-1}) were calculated as:

$$f_{CO_2} = \left(\frac{sV}{mVS}\right) t \quad (2)$$

where s is the accumulation rate of gas in the chamber in µatm min^{-1}; V the volume of the chamber in l; S the surface area of the chamber in m^2; mV (in l mol^{-1}) the molar volume of CO_2 at the current atmospheric pressure; and t is a conversion factor from minutes to day. To calculate the CO_2 diffusive gas transfer velocity (k_{CO_2}), we inverted the equation for Fick's law of gas diffusion:

$$k_{CO_2} = \frac{f_{CO_2}}{k_H(p_{CO_{2water}} - p_{CO_{2air}})} \quad (3)$$

where k_{CO_2} is expressed in m d^{-1}; f_{CO_2} is the measured CO_2 flux between the surface water and the atmosphere in the floating chamber, k_H is Henry's constant adjusted for salinity and temperature and $p_{CO_{2water}}$ and $p_{CO_{2air}}$ are the CO_2 partial pressure in the surface water and atmosphere respectively (in µatm). We then calculated k_{N_2O} on the basis of k_{CO_2} using the Schmidt number of both N_2O and CO_2 (Sc_{N_2O} and Sc_{CO_2}) as follows[25]:

$$k_{N_2O} = \left(\frac{Sc_{N_2O}}{Sc_{CO_2}}\right)^{0.67} k_{CO_2} \quad (4)$$

Chemical analyses. Ambient temperature (°C), pH and DO were measured with an environmental probe (YSI, Model 600XLM) equipped with a rapid pulse DO probe. TP was measured by spectrophotometry using the standard molybdenum blue method after persulphate digestion[26]. TN analysis was performed by alkaline persulphate digestion to NO_3^-, subsequently measured on an Alpkem Flow Solution IV autoanalyser. To determine NH_4^+ and NO_3^- concentrations, water was filtered at 0.22 µm and analysed according to the Lachat autoanalyser methods 10-107-06-1-J and 10-107-04-1-C, respectively. The method for NH_4^+ analysis is based on a reaction of ammonia with alkaline phenol and sodium hypochlorite to form indophenol blue, which is subsequently measured by spectrophotometry. NO_3^- concentration was also measured by spectrophotometry after reduction to NO_2^- by a copper-coated cadmium column. Water filtered at 0.45 µm was used for DOC analysis with a Total Organic Carbon analyser 1010-OI following sodium persulphate digestion (OI Analytical, College Station, Texas, USA). Chlorophyll *a* was analysed through spectrophotometry following filtration on Whatman (GF/F) filters and extraction by hot ethanol (90%; ref. 27).

Statistical analysis. To meet normality assumption, all variables were standardized when necessary by using log, square root or square transformations. We also carried out multiple regression analysis with forward selection of the variables for each type of system separately and with all data combined. No multiple regression relationships emerged as significant at a threshold of p-value = 0.05. Overall few relationships were significant in linear regression, and all of these were weak, explaining less than 13% of the variability in N_2O fluxes (Supplementary Table 4).

To explore possible nonlinear interactions, we performed a classification tree analysis to predict the direction of N_2O flux (positive or negative) as a function of different environmental variables (R package 'mvpart'). This nonparametric analysis allows the detection of nonlinear links and interaction effects without being affected by the data distribution. Systems were sorted into two groups (sinks and sources) according to the direction of their N_2O flux. For a better differentiation of the two groups, we decided not to consider systems close to equilibrium in terms of N_2O concentration—that is, with absolute values of $\Delta N_2O < 0.1$ nmol l^{-1}. The trees with the lowest cross-validated relative error (CVRE) were selected on the basis of a 100-fold cross-validation. The two resulting tree-based models presented in Fig. 2b,d explained 27 and 40% of the variability with cross-validated relative errors (CVRE) of 0.77 and 0.74, respectively. In view of the high CVRE of these models, we used a Kendall rank correlation test to confirm statistical significance of the link between N_2O flux direction and the environmental factors selected in the trees. For the first tree (Fig. 2b), we tested the correlation between lake flux direction and pH, which seemed very significant with a p-value < 0.001. We then tested the correlation between flux direction and DOC on lakes with pH < 6.275 (which corresponds to the second node of the tree), and also obtained a significant result with a p-value = 0.002. The same method was used to test the node in the second tree (Fig. 2d) and resulted in a significant link between flux direction and DO, with a p-value = 0.004. However, given the high CVRE, the models are more suggestive than predictive, and, therefore, should be interpreted and used with caution.

Geographical analysis. Spatial analyses were performed on ArcMap GIS 10.0 using the National Hydro Network data[28] with a resolution of 1:50 000. Regional delimitations contained drainage areas of all sampled sites. Lake and pond area per region was calculated by separating the polygons based on a size criterion of 0.01 km^2 (considering smaller as ponds). Streams and rivers are digitized as segments in the National Hydro Network map. To determine regional lotic area, we first calculated Strahler stream order for all rivers in the aquatic network, based on a digital elevation model interpolation using the ArcMap GIS 10.0 Strahler order tool. We then calculated the total length for each river order and multiplied it by a specific width. Average widths were measured from sampled sites of the corresponding order in each region. When river width was not available for a given river order in a region, we used the formula in ref. 29 to derive it based on modelled global constants.

Regional budgets. To calculate annual aquatic N_2O emissions for the Saguenay region, we compiled mean seasonal flux rates for each type of system. We considered gas exchange with the atmosphere to be null during the ice-covered season. We divided the ice-free period into three components: spring (from ice-out to 20 June), summer (from 21 June to 20 September), and fall (from 21 September to 1 January). Mean spring emissions were calculated as the sum of: the estimated outgassing of winter-derived N_2O accumulated under-ice; the average of fluxes measured in April applied to the period of 16 April to 30 April; and the average of fluxes measured in June and applied to the rest of the spring period. The N_2O winter accumulation under the ice was estimated assuming a linear build-up of this gas throughout the winter, based on the observed increase of N_2O between the end of the fall, and the mid-winter under-ice N_2O concentration. We assumed that all the N_2O in excess accumulated under the ice throughout the winter was emitted to the atmosphere at ice thaw. To derive a regional estimate of aquatic N_2O flux (Table 2), we multiplied mean seasonal or annual areal N_2O fluxes of lakes, ponds and rivers by the proportion of area covered by each of these types of system in the region.

Global budget. To calculate global emissions of N_2O from lakes, reservoirs, rivers and streams, we compiled literature values of surface water–atmospheric fluxes derived directly from field studies (Supplementary Tables 5 and 6). When a system

was sampled at several sites or at several times, we used an average of the reported fluxes to derive a single value that incorporates as much as possible the intrinsic flux variability of the system. We reported aggregated averages of fluxes for studies on a large number of systems or when individual values were not available. When only a range of fluxes was available, we considered the mean of the range as an average flux. Data were sorted according to three broad latitudinal ranges corresponding to high latitudes (higher than 54°), temperate (between 24° and 54°), and tropical (lower than 24°) regions. Based on values reported in Supplementary Tables 5 and 6, averages were calculated for lentic (lakes and reservoirs) and lotic (streams and rivers) ecosystems for each section of the globe (by accounting for the number of systems). To estimate global annual emissions, latitudinal averages were upscaled to the corresponding lentic and lotic surface areas reported in ref. 30. The global estimate incorporating results from this study (Table 3) was calculated by replacing literature values for latitudes >54° by our own. Mean flux rates from Côte-Nord and Saguenay were used to calculate a lower and upper bound, respectively, and values from all three regions sampled were used to derive an average flux.

References

25. Cole, J. J. & Caraco, N. F. Atmospheric exchange of carbon dioxide in a low-wind oligotrophic lake measured by the addition of SF6. *Limnol. Oceanogr.* **43,** 647–656 (1998).
26. Cattaneo, A. & Prairie, Y. T. Temporal variability in the chemical characteristics along the Rivière de l'Achigan: How many samples are necessary to describe stream chemistry? *Can. J. Fish. Aquat. Sci.* **52,** 828–835 (1995).
27. Nusch, E. Comparison of different methods for chlorophyll and phaeopigment determination. *Arch. Hydrobiol. Beih.* **14,** 14–36 (1980).
28. *National Hydro Network* (Natural Resources Canada, accessed 19 November 2015); http://geogratis.gc.ca/api/en/nrcan-rncan/ess-sst/-/(urn:iso:series)geobase-national-hydro-network-nhn?sort-field=relevance
29. Downing, J. A. *et al.* Global abundance and size distribution of streams and rivers. *Inland Wat.* **2,** 229–236 (2012).
30. Bastviken, D., Tranvik, L. J., Downing, J. A., Crill, P. M. & Enrich-Prast, A. Freshwater methane emissions offset the continental carbon sink. *Science* **331,** 50 (2011).